International Journal of Solids and Structures 48 (2011) 3020–3031

Contents lists available at ScienceDirect

International Journal of Solids and Structures

journal homepage: www.elsevier.com/locate/ijsolstr

Periodic crack problem for a functionally graded half-plane an analytic solution

Bora Yıldırım [a], Özge Kutlu [b], Suat Kadıoğlu [c,*]

[a] Hacettepe University, Mechanical Engineering Dept., 06800 Ankara, Turkey
[b] Aselsan Inc., Mechanical Design Dept., 06172 Ankara, Turkey
[c] Middle East Technical University, Mechanical Engineering Dept., 06800 Ankara, Turkey

ARTICLE INFO

Article history:
Received 2 March 2011
Received in revised form 27 June 2011
Available online 1 July 2011

Keywords:
Fracture
Functionally graded
Integral equation
Multiple crack
Stress intensity factor
Thermal stress

ABSTRACT

The plane elasticity problem of a functionally graded semi-infinite plane, containing periodic imbedded or edge cracks perpendicular to the free surface is considered. Cracks are subjected to mode one mechanical or thermal loadings, which are represented by crack surface tractions. Young's modulus, conduction coefficient, coefficient of thermal expansion are taken as exponentially varying functions of the depth coordinate where as Poisson ratio and thermal diffusivity are assumed to be constant. Fourier integrals and Fourier series are used in the formulation which lead to a Cauchy type singular integral equation. The unknown function which is the derivative of crack surface displacement is numerically solved and used in the calculation of stress intensity factors. Limited finite element calculations are done for verification of the results which demonstrate the strong dependence of stress intensity factors on geometric and material parameters.

1. Introduction

Functionally graded materials (FGMs) are nontraditional engineering materials that are used especially in coating applications such as thermal barrier or wear resistant coatings (Erdogan, 1995). They are inhomogeneous materials whose properties vary in a specified manner. In order to gain a better understanding of the fracture of functionally graded materials, different researchers have solved many crack problems associated with FGMs within the last couple of decades. Employing various material modeling approaches and solution techniques, many useful results have been obtained for different crack configurations and loading conditions. There exist now, a vast literature on this subject. A relatively less studied subject within this vast literature pertains to the periodic cracking of functionally graded materials.

In this study one such problem, namely, plane strain mode one periodic cracking of a functionally graded semi-infinite plane is considered. Granted, the problem at hand is a highly idealized one and even more realistic problems (such as an FGM coating bonded to a half plane) have already been solved as will be discussed in the forthcoming literature survey. The distinguishing feature of this study, however, is that an analytical solution with a certain subtlety (to be discussed in Section 2) is being presented. In the earlier studies, either finite element or some other approximate method is used; or analytical solutions are obtained for some special materials which have variable thermal properties but constant elastic properties. Hence to the best of authors' knowledge, the analytical solution to the problem presented here, has not been published yet. The relevant literature is briefly reviewed in the following. The scope of the literature survey is restricted to periodic crack problems in linear elastic materials under thermal or mechanical loads.

Periodic cracks in homogeneous materials are investigated by many researchers. Earliest works belong to Benthem and Koiter (1973), and Bowie (1973) who solved the problem of a half-plane with periodic edge cracks by using different approaches. Nisitani et al. (1973) considered a row of internal cracks in a semi-infinite plane under uniform tension. Nemat-Nasser et al. (1978) addressed the issue of stability of crack growth under specific thermal stress conditions by considering a half plane containing two sets of interacting periodic edge cracks which are equally spaced but of unequal lengths. Stress intensity factors (SIF) used in the stability analysis are obtained from the solution of a singular integral equation with Cauchy type singularity. Isida (1979) also considered an array of parallel edge cracks in a semi-infinite plane under uniform tension. Some results from Nisitani et al. (1973) and Isida (1979) are given in Murakami (1987). Nied (1987) considered the elasticity problem of an infinite array of periodic internal cracks in a half plane, such that edge cracks could also be obtained as a special case. Dependence of SIFs and crack opening displacements on crack spacing has been investigated. In Nied (1987), instead of taking the usual approach of formulating the problem by using the derivative of the crack surface displacement (which leads to a singular integral equation

* Corresponding author. Tel.: +90 312 210 5294; fax: +90 312 210 2536.
E-mail addresses: boray@hacettepe.edu.tr (B. Yıldırım), ozunal@aselsan.com.tr (Ö. Kutlu), kadioglu@metu.edu.tr (S. Kadıoğlu).

0020-7683/$ - see front matter © 2011 Elsevier Ltd. All rights reserved.
doi:10.1016/j.ijsolstr.2011.06.019

of the Cauchy type), an alternative approach has been followed in which the unknown function is taken to be the crack surface displacement, and this approach results in a hypersingular integral equation. The problem was formulated first, for a single crack by using Fourier transforms and then the expressions for multiple cracks were obtained by using superposition. Later, Schulze and Erdogan (1998) considered the periodic cracking of a homogeneous elastic coating bonded to a homogeneous substrate. They expressed the displacement field in the cracked medium as the superposition of Fourier integrals and Fourier series and formulated the problem in terms of the crack surface displacement, which led to a hypersingular integral equation.

Thermal stress problems for homogeneous media containing periodic cracks have been considered by Rizk (2003, 2005, 2006) in a series of articles. In Rizk (2003) periodic cracks in a half-plane which is subjected to convective cooling is considered. The thermal stress problem for the crack free medium was solved first and then the thermal stresses with the opposite sign were applied as the crack surface tractions. The problem was formulated for a single crack by using Fourier transforms and the derivative of crack surface displacement as the unknown function. Superposition was used to obtain the required expressions for multiple cracks as in Nied (1987) and a singular integral equation with Cauchy type singularity was obtained. In Rizk (2005) and Rizk (2006) different periodic crack configurations in elastic strips have been considered. In these studies, the problems were formulated by using Fourier series and Fourier Integrals in terms of the crack surface displacements, which led to hypersingular integral equations. In all of these studies transient SIFs have been presented. Multiple cracking of an elastic homogeneous coating under transient thermal load has been addressed by Wang and Mai (2007). In Schulze and Erdogan (1998) and Wang and Mai (2007), the overall geometry of the cracked body and the solution methods were the same, the only difference being the applied loading. A more recent contribution in this area came from Jin and Feng (2009), where a homogeneous elastic strip containing an array of parallel edge cracks with alternating lengths subjected to a thermal shock, is considered. A Fourier transform-superposition method, similar to that in Rizk (2003) was used, which led to a system of singular integral equations (Cauchy type) for the unknown crack surface displacement derivatives. Thermal SIFs were presented.

In all of the studies reviewed so far plane strain or plane stress solutions were obtained.

Since mid 1990's, solutions to periodic crack problems in functionally graded materials have started to appear in the technical literature. Two main venues followed by the researchers to obtain solutions are the integral equation method and the finite element method (FEM). Here, the analytical solutions are reviewed first in some detail. Finite element studies will be briefly mentioned next.

Periodic cracking of a functionally graded coating bonded to a homogeneous substrate under anti-plane loading has been considered by Erdogan and Ozturk (1995). Functional grading was represented as an exponentially varying modulus of rigidity. A hypersingular integral equation whose unknown is the crack surface displacement, was derived and mode III SIFs, stresses, crack opening displacements and strain energy released per unit surface area were calculated. Later Chen (2006) and, Wang and Mai (2006a) also considered anti-plane problem of periodic cracks in graded coatings but for transient (dynamic) loading. In both of these articles, time dependence had been taken care of by using Laplace transforms, and hypersingular integral equations are obtained by using Fourier transforms and Fourier series for unknown crack surface displacements. Recently, anti-plane problem of periodic interface cracks in a functionally graded coating-substrate structure has been considered by Ding and Li (2008).

Choi (1997) considered periodic imbedded cracks in an infinite non-homogeneous medium loaded under in-plane normal and shear stresses. The non-homogeneity is represented as an exponentially varying modulus of rigidity in the direction of the cracks, whereas Poisson ratio is taken as constant. Hypersingular integral equations (whose unknowns are the crack surface displacements) for each individual loading mode are derived and solved. SIFs and crack surface displacements have been presented. Later, Wang and Mai considered the same kind of material parameter variation and crack configuration for the cases of thermo-mechanical (Wang and Mai, 2005) and transient (dynamic) loading (Wang and Mai, 2006b). In an earlier study, Afsar and Sekine (2000) discussed the effect of crack spacing on the brittle fracture characteristics of a semi-infinite functionally graded material with periodic edge cracks. Their approach to material modeling, however, has been quite different. Quoting, "The non-homogeneity of the material is simulated by an equivalent eigenstrain, whereby the problem is reduced to that of a cracked homogeneous material with incompatible and equivalent eigenstrains." Recently, Jin and Feng considered multiple edge crack problems under thermal shock for a thermally graded but elastically homogeneous plate (Jin and Feng, 2008a) and for a thermally graded but elastically homogeneous coating on a homogeneous substrate (Jin and Feng, 2008b). Feng and Jin (2009) also considered thermal fracture of a thermally graded but elastically homogeneous plate containing two sets of interacting periodic edge cracks which are equally spaced but of unequal lengths. In all of these studies, a Fourier transform-superposition method similar to those in Nied (1987) and (Rizk, 2003) are used and, the unknown being the crack surface displacement derivative, singular integral equations with Cauchy type singularity are obtained. Thermal SIFs were calculated and predictions regarding thermal shock resistance were made.

Periodic crack problems in functionally graded materials have also been addressed by using FEM. Thermal and mechanical loading of coating-substrate systems (Bao and Wang, 1995), thermal loading with temperature dependent material parameters (Ueda, 2002), thermal shock enhancement due to multiple cracking (Han and Wang, 2006) and three dimensional crack problems (Dag et al., 2008) have been considered.

The current study presents the analytic solution of plane strain mode one periodic crack problem of a functionally graded semi-infinite plane. Spatial variation of the Young's modulus is taken as an exponential function, and Poisson ratio is taken as constant. The problem has been reduced to a perturbation problem in which the crack surface tractions are the only non-zero external loads. Following (Schulze and Erdogan, 1998), a Fourier integral-Fourier series representation of displacements is used in the formulation, but a Cauchy type singular integral equation is derived since the auxiliary unknown function is selected as the derivative of the crack surface displacement rather than the displacement. In this respect, the given solution is unique considering the literature survey given above. The analytic approach developed here can be extended to more realistic cases such as functionally graded strips or coatings containing periodic cracks. The main objective of this study is to examine the effect of length parameters (i.e. crack location, spacing and crack length) and material grading on SIFs for imbedded and edge cracks. SIFS are given for general loading conditions as well as constant strain and thermal shock loadings.

2. Formulation of the problem

The geometry of the plane elasticity problem of periodic cracks in a functionally graded semi-infinite medium is given in Fig. 1. By

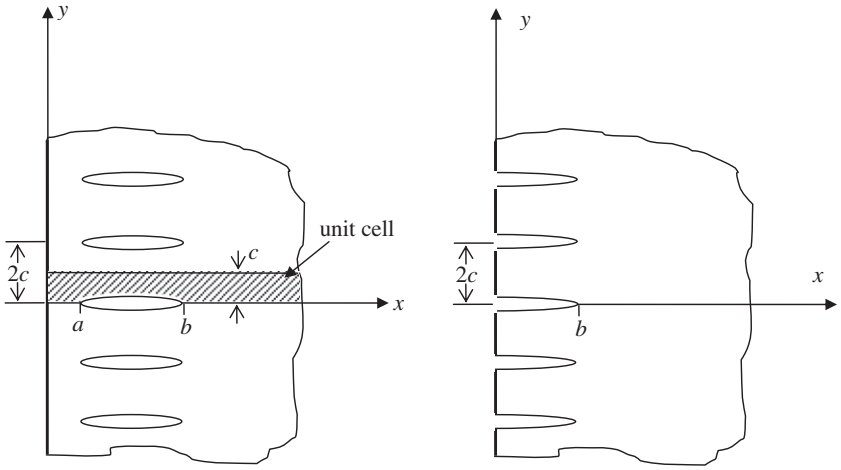

Fig. 1. Geometry of the problem.

extending the cracks to the stress-free boundary, the problem of periodic edge cracks can also be obtained. Shear modulus varies along x-direction as an exponential function.

$$\mu(x) = \mu_0 \exp(\beta x) \tag{1}$$

where β is the nonhomogeneity constant, and μ_0 is the modulus of rigidity at $x = 0$. Following (Choi, 1997), Poisson ratio v is taken as constant. In order to unify plane stress and plane strain formulations, Kolosov constant is used which is defined as

$$\kappa = 3 - 4v \tag{2}$$

for plane strain and

$$\kappa = \frac{3 - v}{1 + v} \tag{3}$$

for plane stress. By using equilibrium equations and stress–strain relationships, the governing equations in terms of the displacements can be expressed as follows:

$$(\kappa+1)\frac{\partial^2 u}{\partial x^2} + (\kappa-1)\frac{\partial^2 u}{\partial y^2} + 2\frac{\partial^2 v}{\partial x \partial y} + \beta(\kappa+1)\frac{\partial u}{\partial x} + \beta(3-\kappa)\frac{\partial v}{\partial y} = 0, \tag{4.a}$$

$$(\kappa-1)\frac{\partial^2 v}{\partial x^2} + (\kappa+1)\frac{\partial^2 v}{\partial y^2} + 2\frac{\partial^2 u}{\partial x \partial y} + \beta(\kappa-1)\frac{\partial u}{\partial y} + \beta(\kappa-1)\frac{\partial v}{\partial x} = 0. \tag{4.b}$$

The assumed form of solution which has the capacity to satisfy (4) and the boundary conditions is as follows (Schulze and Erdogan, 1998):

$$u(x,y) = \frac{1}{2\pi}\int_{-\infty}^{\infty} U_1(y,\rho)e^{-ix\rho}d\rho + \sum_{n=0}^{\infty} U_2(x,\alpha_n)\cos(y\alpha_n), \tag{5.a}$$

$$v(x,y) = \frac{1}{2\pi}\int_{-\infty}^{\infty} V_1(y,\rho)e^{-ix\rho}d\rho + \sum_{n=0}^{\infty} V_2(x,\alpha_n)\sin(y\alpha_n), \tag{5.b}$$

where

$$\alpha_n = \frac{n\pi}{c}. \tag{5.c}$$

By substituting (5) into (4), one can find

$$U_1 = m_1 A_1(\rho)e^{n_1 y} + m_2 A_2(\rho)e^{n_2 y} + m_3 A_3(\rho)e^{n_3 y} + m_4 A_4(\rho)e^{n_4 y} \tag{6.a}$$

$$V_1 = A_1(\rho)e^{n_1 y} + A_2(\rho)e^{n_2 y} + A_3(\rho)e^{n_3 y} + A_4(\rho)e^{n_4 y} \tag{6.b}$$

where

$$n_1 = -\frac{1}{2}\cdot\beta\sqrt{\frac{3-\kappa}{\kappa+1}} - \frac{1}{2}\cdot\sqrt{4\rho^2 + 4i\beta\rho + \beta^2\frac{3-\kappa}{\kappa+1}}, \tag{7.a}$$

$$n_2 = \frac{1}{2}\cdot\beta\sqrt{\frac{3-\kappa}{\kappa+1}} - \frac{1}{2}\cdot\sqrt{4\rho^2 + 4i\beta\rho + \beta^2\frac{3-\kappa}{\kappa+1}}, \tag{7.b}$$

$$n_3 = -\frac{1}{2}\cdot\beta\sqrt{\frac{3-\kappa}{\kappa+1}} + \frac{1}{2}\cdot\sqrt{4\rho^2 + 4i\beta\rho + \beta^2\frac{3-\kappa}{\kappa+1}}, \tag{7.c}$$

$$n_4 = \frac{1}{2}\cdot\beta\sqrt{\frac{3-\kappa}{\kappa+1}} + \frac{1}{2}\cdot\sqrt{4\rho^2 + 4i\beta\rho + \beta^2\frac{3-\kappa}{\kappa+1}}, \tag{7.d}$$

$$m_j = \frac{(\kappa-1)\cdot(\rho^2 + i\rho\beta) - (\kappa+1)n_j^2}{(\beta(\kappa-1) - 2i\rho)n_j}, \quad (j = 1,\ldots,4); \tag{8}$$

and

$$U_2 = q_1 B_{1n}(\alpha_n)e^{p_1 x} + q_2 B_{2n}(\alpha_n)e^{p_2 x}, \tag{9.a}$$

$$V_2 = B_{1n}(\alpha_n)e^{p_1 x} + B_{2n}(\alpha_n)e^{p_2 x}, \tag{9.b}$$

where,

$$p_1 = -\frac{\beta}{2} - \frac{1}{2}\cdot\sqrt{\beta^2 + 4\alpha_n^2 + i4\beta\alpha_n}\cdot\sqrt{\frac{3-\kappa}{\kappa+1}}, \tag{10.a}$$

$$p_2 = -\frac{\beta}{2} - \frac{1}{2}\cdot\sqrt{\beta^2 + 4\alpha_n^2 - i4\beta\alpha_n}\cdot\sqrt{\frac{3-\kappa}{\kappa+1}}, \tag{10.b}$$

$$q_j = \frac{(\kappa-1)p_j(p_j+\beta) - \alpha_n^2(\kappa+1)}{\alpha_n(2p_j + \beta(\kappa-1))}, \quad (j = 1,2). \tag{11}$$

Note that in (9), the boundedness of displacements U_2 and V_2 as $x \to \infty$ has been taken into account. Then the displacements and (by using stress-strain relationships) the stresses can be written as;

$$u(x,y) = \frac{1}{2\pi}\int_{-\infty}^{\infty}\sum_{j=1}^{4} m_j(\rho)\cdot A_j(\rho)\cdot e^{n_j y - ix\rho}d\rho + \sum_{n=0}^{\infty}\sum_{j=1}^{2} q_j(\alpha_n)\cdot B_{jn}(\alpha_n)\cdot e^{p_j x}\cdot\cos(y\alpha_n), \tag{12.a}$$

$$v(x,y) = \frac{1}{2\pi}\int_{-\infty}^{\infty}\sum_{j=1}^{4} A_j(\rho)\cdot e^{n_j y - ix\rho}d\rho + \sum_{n=0}^{\infty}\sum_{j=1}^{2} B_{jn}(\alpha_n)\cdot e^{p_j x}\cdot\sin(y\alpha_n). \tag{12.b}$$

$$\sigma_{xx}(x,y)=\frac{\mu(x)}{\kappa-1}\left[\frac{1}{2\pi}\int_{-\infty}^{\infty}\sum_{j=1}^{4}[(3-\kappa)n_j(\rho)-i\rho(\kappa+1)m_j(\rho)]\cdot A_j(\rho)\cdot e^{n_jy-ix\rho}d\rho+\sum_{n=0}^{\infty}\sum_{j=1}^{2}[(\kappa+1)\cdot p_j(\alpha_n)\cdot q_j(\alpha_n)+(3-\kappa)\cdot\alpha_n]\cdot B_{jn}(\alpha_n)\cdot e^{p_jx}\cdot\cos(y\alpha_n)\right], \tag{13.a}$$

$$\sigma_{yy}(x,y)=\frac{\mu(x)}{\kappa-1}\left[\frac{1}{2\pi}\int_{-\infty}^{\infty}\sum_{j=1}^{4}[(\kappa+1)n_j(\rho)-i\rho(3-\kappa)m_j(\rho)]\cdot A_j(\rho)\cdot e^{n_jy-ix\rho}d\rho+\sum_{n=0}^{\infty}\sum_{j=1}^{2}[(3-\kappa)\cdot p_j(\alpha_n)\cdot q_j(\alpha_n)+(\kappa+1)\cdot\alpha_n]\cdot B_{jn}(\alpha_n)\cdot e^{p_jx}\cdot\cos(y\alpha_n)\right], \tag{13.b}$$

$$\sigma_{xy}(x,y)=\mu(x)\left[\frac{1}{2\pi}\int_{-\infty}^{\infty}\sum_{j=1}^{4}[m_j(\rho)\cdot n_j(\rho)-i\rho]\cdot A_j(\rho)\cdot e^{n_jy-ix\rho}d\rho+\sum_{n=0}^{\infty}\sum_{j=1}^{2}[p_j(\alpha_n)-\alpha_n\cdot q_j(\alpha_n)]\cdot B_{jn}(\alpha_n)\cdot e^{p_jx}\cdot\sin(y\alpha_n)\right]. \tag{13.c}$$

In the expressions above there are two groups of unknown functions (A_1,A_2,A_3,A_4 and B_{1n},B_{2n}) which are supposed to be determined by using the boundary conditions. Since the solution is periodic, it is sufficient to consider a semi-infinite strip along x-axis such that $0\leqslant y\leqslant c$. In Fig. 1, the domain of the elastic solution is shaded. It is assumed that through an appropriate superposition, the elasticity problem is reduced to a perturbation problem where the only non-zero loads are the self-equilibriating crack surface tractions. The boundary conditions of the problem are then given as follows:

$$v(x,0)=0,\quad 0<x<a\quad\text{and}\quad b<x<\infty, \tag{14.a}$$
$$\sigma_{yy}(x,0)=-p(x),\quad a<x<b, \tag{14.b}$$
$$\sigma_{xy}(x,0)=0,\quad 0<x<\infty, \tag{14.c}$$
$$\sigma_{xy}(x,c)=0,\quad 0<x<\infty, \tag{14.d}$$
$$v(x,c)=0,\quad 0<x<\infty, \tag{14.e}$$
$$\sigma_{xx}(0,y)=0,\quad 0<y<c, \tag{14.f}$$
$$\sigma_{xy}(0,y)=0,\quad 0<y<c, \tag{14.g}$$

Of these conditions, (14.a,b) are the mixed boundary conditions. Conditions (14.a), and (14.c-e) enforce periodic solution with respect to $y=nc$ ($n=0,1,2,\ldots$). These conditions are readily satisfied by the Fourier series because of $sin(y\alpha_n)$ term. Conditions (14.f) and (14.g) are the stress free boundary conditions for the half plane.

The derivative of crack surface displacement is going to be used as the auxiliary unknown in terms of which the other unknowns will be expressed. Defining

$$g(x)=\frac{\partial v(x,0)}{\partial x},\quad 0<x<\infty, \tag{15}$$

and using the homogeneous boundary conditions (14.a), and (14.c-e), one can obtain A_1, A_2, A_3 and A_4, after rather lengthy manipulations as follows:

$$A_1=\frac{(e^{2Ac}-e^{2Bc})}{2\{\cosh(2Ac)-\cosh(2Bc)\}}\frac{(m_2n_2-i\rho)}{(m_2n_2-m_1n_1)}\frac{i}{\rho}\int_a^b e^{it\rho}g(t)dt, \tag{16.a}$$

$$A_2=\frac{(e^{2Bc}-e^{-2Ac})}{2\{\cosh(2Ac)-\cosh(2Bc)\}}\frac{(m_1n_1-i\rho)}{(m_2n_2-m_1n_1)}\frac{i}{\rho}\int_a^b e^{it\rho}g(t)dt, \tag{16.b}$$

$$A_3=\frac{(e^{-2Bc}-e^{2Ac})}{2\{\cosh(2Ac)-\cosh(2Bc)\}}\frac{(m_1n_1-i\rho)}{(m_2n_2-m_1n_1)}\frac{i}{\rho}\int_a^b e^{it\rho}g(t)dt, \tag{16.c}$$

$$A_4=\frac{(e^{-2Ac}-e^{-2Bc})}{2\{\cosh(2Ac)-\cosh(2Bc)\}}\frac{(m_2n_2-i\rho)}{(m_2n_2-m_1n_1)}\frac{i}{\rho}\int_a^b e^{it\rho}g(t)dt, \tag{16.d}$$

where,

$$A=\frac{\beta}{2}\sqrt{\frac{3-\kappa}{\kappa+1}},\quad B=\frac{1}{2}\sqrt{4\rho^2+4i\beta\rho+\beta^2\frac{3-\kappa}{\kappa+1}}. \tag{17}$$

Here, one should be aware of the fact that, since the auxiliary function that is being used is the derivative of the crack surface displacement, boundary condition (14.a) and therefore Eq. (12.b) has been differentiated with respect to x. So at this point, with A_i ($i=1,2,3,4$) given above, the condition

$$\frac{\partial v(x,0)}{\partial x}=0,\quad 0<x<a\quad\text{and}\quad b<x<\infty, \tag{18}$$

is satisfied rather than the actual boundary condition (14.a) itself. This is the subtlety which was mentioned earlier in Section 1. Further effort will be required to remedy this situation. This issue however will be addressed in Section 3.

Now, since the unknown functions A_1, A_2, A_3 and A_4 are determined in terms of $g(t)$, one can turn to the question of finding $B_{1n}(\alpha_n)$ and $B_{2n}(\alpha_n)$.

Applying boundary condition (14.f) along with (13.a), one can obtain

$$\frac{1}{2\pi}\int_{-\infty}^{\infty}\sum_{k=1}^{4}L_kA_ke^{n_ky}d\rho+\sum_{n=0}^{\infty}\sum_{k=1}^{2}M_kB_{kn}\cos(y\alpha_n)=0 \tag{19}$$

where

$$L_k=(3-\kappa)n_k-i\rho(\kappa+1)m_k,\quad(k=1,\ldots,4) \tag{20.a}$$
$$M_k=(\kappa+1)p_kq_k+(3-\kappa)\alpha_n.\quad(k=1,2) \tag{20.b}$$

Now recalling the orthogonality relationship for cosine function one can multiply both sides of Eq. (19) with $\cos(y\alpha_m)dy$ and integrate $y\in(0,c)$.

By doing so all the terms in the infinite series vanish except $n=m$. Integrating the first term twice, (first over $y\in(0,c)$ by using standard integration techniques, and then, after substituting $A_k(\rho)$ from (16), over $\rho\in(-\infty,\infty)$ by using contour integration on the complex plane) Eq. (19) can be written as follows:

$$G_1+\sum_{k=1}^{2}M_kB_{km}\hat{c}_m=0,\quad(m=0,1,2,3\ldots) \tag{21}$$

where, $\hat{c}_m=c$ if $m=0$, and $\hat{c}_m=c/2$ when $m\neq0$. G_1 is given as;

$$G_1=-\frac{4i(\kappa-1)\alpha_m^2}{\pi(\kappa+1)}\int_a^b g(t)I(t)dt, \tag{22}$$

where

$$I(t)=\frac{2\pi}{\lambda_1}\left[\lambda_4\left(1-\frac{\beta}{\lambda_2}\right)+\lambda_5\left(-1+\frac{\beta}{\lambda_3}\right)\right], \tag{23.a}$$

$$\lambda_1=4\alpha_m\beta\sqrt{\frac{3-\kappa}{1+\kappa}},\quad\lambda_2=\sqrt{4\alpha_m^2+\beta^2-i\lambda_1}, \tag{23.b}$$

$$\lambda_3=\sqrt{4\alpha_m^2+\beta^2+i\lambda_1},\quad\lambda_4=\exp\left[(\beta-\lambda_2)\frac{t}{2}\right],\quad\lambda_5=\exp\left[(\beta-\lambda_3)\frac{t}{2}\right]. \tag{23.c}$$

Similarly, applying boundary condition (14.g) along with (13.c), and defining

$$R_k=m_k\cdot n_k-i\rho,\quad(k=1,\ldots,4) \tag{24.a}$$
$$S_k=p_k-\alpha_n\cdot q_k,\quad(k=1,2) \tag{24.b}$$

one obtains

$$\frac{1}{2\pi}\int_{-\infty}^{\infty}\sum_{k=1}^{4}R_k\cdot A_k\cdot e^{n_j y}d\rho+\sum_{n=0}^{\infty}\sum_{k=1}^{2}S_k\cdot B_{kn}\cdot\sin(y\alpha_n)=0. \tag{25}$$

Proceeding similarly, one can multiply both sides of Eq. (25) with $\sin(y\alpha_m)dy$ and integrate $y\in(0,c)$. Then again, all the terms in the series summation vanish except for $n=m$. As before, the first term is integrated twice, first over $y\in(0,c)$ and then over $\rho\in(-\infty,\infty)$ after substituting $A_k(\rho)$ from (16). This leads to

$$G_2+\sum_{k=1}^{2}S_kB_{km}c'_m=0.\quad(m=0,1,2,3\ldots) \tag{26}$$

where $c'_m=0$ if $m=0$, and $c'_m=c/2$ when $m\neq 0$. G_2 is given as;

$$G_2=\frac{-4\alpha_m^2}{\lambda_1(\kappa+1)}\int_a^b g(t)\hat{I}(t)dt, \tag{27}$$

where

$$\hat{I}(t)=-\pi i\frac{i\alpha_m+\beta\sqrt{\frac{3-\kappa}{\kappa+1}}}{\left(\lambda_2\beta\sqrt{\frac{3-\kappa}{\kappa+1}}\right)}\lambda_4-\pi i\frac{-i\alpha_m+\beta\sqrt{\frac{3-\kappa}{\kappa+1}}}{\left(\lambda_3\beta\sqrt{\frac{3-\kappa}{\kappa+1}}\right)}\lambda_5. \tag{28}$$

Now, B_{1m}, B_{2m} can be solved from equations (21) and (26), along with (22) and (27) giving;

$$B_{1m}=\int_a^b g(t)\widehat{B}_{1m}dt,\quad B_{2m}=\int_a^b g(t)\widehat{B}_{2m}dt, \tag{29.a}$$

where

$$\widehat{B}_{1m}=\frac{4i\alpha_m\left[M_2\hat{c}_m\hat{I}(t)+(\kappa-1)\alpha_mS_2c'_mI(t)\right]}{\hat{c}_mc'_m\pi(\kappa+1)(M_1S_2-M_2S_1)}, \tag{29.b}$$

$$\widehat{B}_{2m}=\frac{-4i\alpha_m\left[M_1\hat{c}_m\hat{I}(t)+(\kappa-1)\alpha_mS_1c'_mI(t)\right]}{\hat{c}_mc'_m\pi(\kappa+1)(M_1S_2-M_2S_1)}. \tag{29.c}$$

Here, one can show that if $m=\alpha_m=0$ then $B_{1m}=B_{2m}=0$ therefore the Fourier series could be started from one. The remaining boundary condition (14.b) is used along with (13.b), (16) and (29) to obtain the integral equation for the unknown function $g(t)$:

$$\int_a^b(h_1(x,t)+h_2(x,t))g(t)dt=-\frac{p(x)(\kappa-1)}{\mu(x)} \tag{30}$$

In (30),

$$h_1(x,t)=\lim_{y\to 0}\left\{\frac{1}{2\pi}\int_0^{\infty}M(y,\rho)\cos(\rho(t-x))d\rho+\frac{1}{2\pi}\int_0^{\infty}N(y,\rho)\sin(\rho(t-x))d\rho\right\} \tag{31}$$

where

$$M(y,\rho)=K_1(y,\rho)+K_1(y,-\rho), \tag{32.a}$$

$$N(y,\rho)=i(K_1(y,\rho)-K_1(y,-\rho)), \tag{32.b}$$

$$K_1(y,\rho)=\frac{i[K_{11}(y,\rho)-K_{12}(y,\rho)-K_{13}(y,\rho)+K_{14}(y,\rho)]}{2\rho(m_2n_2-m_1n_1)(\cosh(2Ac)-\cosh(2Bc))} \tag{32.c}$$

$$K_{11}(y,\rho)=((\kappa+1)n_1(\rho)-i\rho(3-\kappa)m_1(\rho))(m_2n_2-i\rho)e^{n_1y}(e^{2Ac}-e^{2Bc}), \tag{32.d}$$

$$K_{12}(y,\rho)=((\kappa+1)n_2(\rho)-i\rho(3-\kappa)m_2(\rho))(m_1n_1-i\rho)e^{n_2y}(e^{-2Ac}-e^{2Bc}), \tag{32.e}$$

$$K_{13}(y,\rho)=((\kappa+1)n_3(\rho)-i\rho(3-\kappa)m_3(\rho))(m_1n_1-i\rho)e^{n_3y}(e^{2Ac}-e^{-2Bc}), \tag{32.f}$$

$$K_{14}(y,\rho)=((\kappa+1)n_4(\rho)-i\rho(3-\kappa)m_4(\rho))(m_2n_2-i\rho)e^{n_4y}(e^{-2Ac}-e^{-2Bc}), \tag{32.g}$$

$$h_2(x,t)=\lim_{y\to 0}\left\{\sum_{n=1}^{\infty}K_2(x,t,\alpha_n)\cos(\alpha_ny)\right\} \tag{33}$$

$$K_2(x,t,\alpha_n)=\sum_{j=1}^{2}[(3-\kappa)p_j(\alpha_n)q_j(\alpha_n)+(\kappa+1)\alpha_n]\widehat{B}_{jn}(\alpha_n)e^{p_jx}. \tag{34}$$

In order to solve the integral Eq. (30), singular behaviors of the kernels $h_1(x,t)$ and $h_2(x,t)$ should be determined. Previous studies (see for example, Kadioglu et al., 1998) indicate that, for imbedded crack case the integral equation is singular, with a Cauchy kernel and this kernel can be revealed through an asymptotic analysis of $h_1(x,t)$ as $\rho\to\infty$. In addition to the Cauchy kernel, the singular integral equation has a generalized Cauchy kernel in the case of an edge crack and this kernel can be extracted through an asymptotic analysis of $h_2(x,t)$ as $\alpha_n\to\infty$. The substitution of $y=0$ in the boundary condition should be postponed until the completion of these asymptotic analysis.

Using (7), (8), (17), (31), (32) and performing the asymptotic analysis, the behaviors of $M(y,\rho)$ and $N(y,\rho)$ as $\rho\to\infty$ can be expressed as follows:

$$M^{\infty}(y,\rho)\cong\left[\frac{b_1}{\rho}+\frac{b_3}{\rho^3}+\frac{b_5}{\rho^5}+\frac{b_7}{\rho^7}+\frac{b_9}{\rho^9}+\frac{b_{11}}{\rho^{11}}+O\left(\frac{1}{\rho^{13}}\right)\right]\times e^{-\rho y} \tag{35}$$

$$N^{\infty}(y,\rho)\cong\left[c_0+\frac{c_2}{\rho^2}+\frac{c_4}{\rho^4}+\frac{c_6}{\rho^6}+\frac{c_8}{\rho^8}+\frac{c_{10}}{\rho^{10}}+\frac{c_{12}}{\rho^{12}}+O\left(\frac{1}{\rho^{14}}\right)\right]\times e^{-\rho y} \tag{36}$$

In these expressions, c_i and b_i are functions of κ and β. In theory, extracting the leading terms should be sufficient to render the infinite integrals in (31) convergent. In this study, however, asymptotic expansions up to the orders ρ^{-13} and ρ^{-14} are considered in order to improve the accuracy of the calculations in the numerical solution of the integral equation. The leading terms are given as,

$$b_1=\frac{4\beta(\kappa-1)}{\kappa+1},\quad c_0=\frac{8(\kappa-1)}{\kappa+1}, \tag{37}$$

and the higher order terms which become rather lengthy are not given here. These terms however, are exactly the same as those that one would obtain for a single crack problem as in Kadioglu et al. (1998), and they can be found in Dag (1997).

By using the asymptotic expansions given in (35) and (36), and following a procedure similar to that given in Dag (1997), one can reduce Eq. (31) into a form which displays the (Cauchy type) singular nature of the integral equation and can be readily used in the numerical solution.

$$\begin{aligned}h_1(x,t)\approx&\frac{c_0}{2\pi}\frac{1}{t-x}-\frac{b_1}{2\pi}\log|t-x|-\frac{b_1}{2\pi}(Ci[G(t-x)]\\&-\log|t-x|)+\frac{1}{2\pi}\int_0^F[N(0,\rho)-c_0]\sin(\rho(t-x))d\rho\\&+\frac{1}{2\pi}\int_0^G M(0,\rho)\cos(\rho(t-x))d\rho\\&+\frac{1}{2\pi}\int_F^{\infty}\left[\frac{c_2}{\rho^2}+\frac{c_4}{\rho^4}+\frac{c_6}{\rho^6}+\frac{c_8}{\rho^8}+\frac{c_{10}}{\rho^{10}}+\frac{c_{12}}{\rho^{12}}\right]\sin(\rho(t-x))d\rho\\&+\frac{1}{2\pi}\int_G^{\infty}\left[\frac{b_3}{\rho^3}+\frac{b_5}{\rho^5}+\frac{b_7}{\rho^7}+\frac{b_9}{\rho^9}+\frac{b_{11}}{\rho^{11}}\right]\cos(\rho(t-x))d\rho,\end{aligned} \tag{38}$$

In (38), Ci is the cosine integral. Integration limits F and G should be chosen as sufficiently large numbers such that the differences between the functions (32.a,b) and their respective asymptotic expansions (35), (36) become negligible. The last two integrals

can be evaluated in closed form by using formulae involving Sine and Cosine integrals (Dag, 1997).

Having expressed $h_1(x,t)$ in a form amenable to numerical solution, attention could be turned to $h_2(x,t)$. For embedded crack problems, $h_2(x,t)$ can be readily evaluated by taking the limit in (33) and summing sufficiently many terms, because the series is convergent. Singular behavior of unknown function $g(t)$, however, changes when $x, t \to 0$ in the case of edge cracks($a = 0$). This change is effected by the generalized Cauchy kernel which can be obtained through an asymptotic analysis of the series by letting $\alpha_n \to \infty$ when x and t also simultaneously approach 0. It is known that $g(t)$ is non-singular at the crack mouth. One, however, still needs to do an asymptotic analysis to be able to calculate the kernel $h_2(x,t)$ accurately for small values of x and t during the numerical solution. Performing this asymptotic analysis, one can obtain the following expression for large values of α_n:

$$K_2^{\infty}(x,t,\alpha_n) \approx \left[a_2\alpha_n^2 + a_1\alpha_n + a_0 + \frac{a_{-1}}{\alpha_n}\right]\exp\left[-\alpha_n(t+x) + \frac{\beta(t-x)}{2}\right], \tag{39}$$

In (39), the coefficients a_2, a_1, a_0 and a_{-1} are very lengthy functions of t, x, β, κ and c which were calculated through a lengthy computer code[1] and they are not given here. By using (39), one can express $h_2(x,t)$ as,

$$h_2(x,t) = \lim_{y\to 0}\left\{\sum_{n=1}^{\infty}\left[K_2(x,t,\alpha_n) - K_2^{\infty}(x,t,\alpha_n)\right]\cos(\alpha_n y) + \sum_{n=1}^{\infty}K_2^{\infty}(x,t,\alpha_n)\cos(\alpha_n y)\right\}. \tag{40}$$

First term of (40) can be calculated numerically by taking the limit and then summing the series. Summing is stopped when the terms start to be negligible. On the other hand, the second term of (40) can be obtained in closed form by using the following formulae:

$$S_{-1}(\theta,\eta) = \sum_{n=1}^{\infty}\frac{1}{n}e^{-n\theta}\cos(n\eta) = -\frac{1}{2}\ln(2\cosh(\theta) - 2\cos(\eta)) - \frac{1}{2}\theta, \tag{41.a}$$

$$S_0(\theta,\eta) = \sum_{n=1}^{\infty}e^{-n\theta}\cos(n\eta) = \frac{\sinh(\theta)}{2\cosh(\theta) - 2\cos(\eta)} - \frac{1}{2}, \tag{41.b}$$

$$S_1(\theta,\eta) = \sum_{n=1}^{\infty}ne^{-n\theta}\cos(n\eta) = -\frac{\cosh(\theta)}{2\cosh(\theta) - 2\cos(\eta)} + 2\frac{\sinh^2(\theta)}{(2\cosh(\theta) - \cos(\eta))^2}, \tag{41.c}$$

$$S_2(\theta,\eta) = \sum_{n=1}^{\infty}n^2e^{-n\theta}\cos(n\eta) = \frac{\sinh(\theta)}{2\cosh(\theta) - 2\cos(\eta)} - 6\frac{\cosh(\theta)}{(2\cosh(\theta) - \cos(\eta))^2}Sinh(\theta) + \frac{\sinh^3(\theta)}{(2\cosh(\theta) - 2\cos(\eta))^3}. \tag{41.d}$$

Then $h_2(x,t)$ can be cast into the following form which is suitable for numerical solution.

$$h_2(x,t) \approx \left[a_2\left(\frac{\pi}{c}\right)^2 S_2\left(\frac{\pi(t+x)}{c},0\right) + a_1\frac{\pi}{c}S_1\left(\frac{\pi(t+x)}{c},0\right) + a_0S_0\left(\frac{\pi(t+x)}{c},0\right) + \frac{a_{-1}}{\pi/c}S_{-1}\left(\frac{\pi(t+x)}{c},0\right)\right]\exp\left[\frac{\beta(t-x)}{2}\right] + \sum_{n=1}^{H}\left[K_2(x,t,\alpha_n) - K_2^{\infty}(x,t,\alpha_n)\right], \tag{42}$$

[1] The authors would be glad to share this code with interested readers. Please contact the corresponding author.

where H is an integer large enough for the convergence of series.

By substituting (38) and (42) into (30), and dividing both sides of the equation by c, the singular integral equation can be written in the following form:

$$\frac{1}{\pi}\int_a^b g(t)\left\{\frac{1}{t-x} - \frac{\beta}{2}\log|t-x| + \frac{2\pi}{c_0}e^{\beta(t-x)/2}\sum_{k=-1}^{2}a_k\left(\frac{\pi}{c}\right)^k S_k\left(\pi\frac{t+x}{c},0\right) + k_f(x,t)\right\}dt = -p(x)\frac{1+\kappa}{4\mu(x)}. \tag{43}$$

In (43), the dominant part of the kernel is written explicitly and the contraction $k_f(x,t)$ denotes to the Fredholm kernel which can be inferred from (38) and (42).

3. Zero displacement condition outside the crack

At this point formulation seems to be complete and ripe for numerical solution. But before proceeding with the solution, the issue raised because of implementing boundary condition (18) rather than (14.a) should be resolved. For this, consider the value of displacement $v(x,0)$ in terms of the displacement derivative $g(x) = \frac{\partial v(x,0)}{\partial x}$, where $v(x,0)$ is given as a Fourier Integral. Defining

$$v(x,0) = \frac{1}{2\pi}\int_{-\infty}^{\infty}V(\rho,0)e^{ix\rho}d\rho, \tag{44}$$

one can show that,

$$v(x,0) = \frac{1}{2\pi}\int_{t=-\infty}^{\infty}g(t)\left\{\int_{\rho=-\infty}^{\infty}\frac{e^{i\rho(x-t)}}{i\rho}d\rho\right\}dt. \tag{45}$$

The inner integral in (45) can be recognized as $\pi sgn(x-t)$, hence

$$v(x,0) = \frac{1}{2}\int_{t=-\infty}^{\infty}g(t)sgn(x-t)dt. \tag{46}$$

Now let us express $v(x,0)$ for a given piecewise continuous function $g(x)$, such that $g(x)$ is non-zero in the interval $x \in [a,b]$ and it is equal to zero elsewhere. Considering a point $x_c > b$,

$$v(x_c,0) = \frac{1}{2}\int_{t=a}^{b}g(t)sgn(x_c - t)dt = \frac{1}{2}\int_{t=a}^{b}g(t)dt. \tag{47}$$

It can be observed that for an imbedded crack problem, the single-valuedness condition

$$\int_{t=a}^{b}g(t)dt = 0, \tag{48}$$

would be explicitly enforced in the solution, so the zero displacement boundary condition is exactly satisfied. On the other hand, for an edge crack problem, (48) gives crack mouth opening displacement and the boundary condition (14.a) would not be satisfied. This problem can be taken care of by superposing another solution to the existing one such that the overall solution satisfies all the boundary conditions.

For this purpose, consider the elasticity problem for a semi-infinite FGM strip along x-axis (Fig. 2), whose modulus of rigidity varies in x direction, Poisson ratio is constant, and subjected to the following boundary conditions:

$$v(x,0) = v_0, \quad v(x,c) = 0, \quad 0 < x < \infty \tag{49.a}$$

$$\sigma_{xy}(x,0) = 0, \quad \sigma_{xy}(x,c) = 0, \quad 0 < x < \infty \tag{49.b}$$

$$\sigma_{xx}(0,y) = 0, \quad \sigma_{xy}(0,y) = 0. \quad 0 < y < c \tag{49.c}$$

One can show that, the solution of this problem is given as;

$$\sigma_{xx}=0,\quad \sigma_{xy}=0,\quad \sigma_{yy}=-\frac{8\mu(x)}{1+\kappa}\frac{v_0}{c}, \tag{50}$$

$$\varepsilon_{xx}=\frac{3-\kappa}{1+\kappa}\frac{v_0}{c},\quad \varepsilon_{yy}=-\frac{v_0}{c},\quad \varepsilon_{xy}=0, \tag{51}$$

$$v(x,y)=\frac{v_0}{c}(c-y). \tag{52}$$

For the overall solution, the displacement in y-direction along x-axis must be equal to zero, therefore from (47), (52) and (14.a);

$$v_0=-\frac{1}{2}\int_{t=a}^{b} g(t)dt. \tag{53}$$

Using (53) and (50), one obtains the additional term to be combined with integral Eq. (43) as follows:

$$\sigma_{yy}=\frac{4\mu(x)}{c(1+\kappa)}\int_{t=a}^{b} g(t)dt. \tag{54}$$

Then, from (54) one can easily see that, the only modification needed in (43) is to add $\frac{\pi}{c}$ to the Fredholm kernel $k_f(x,t)$, so that the singular integral equation of the problem becomes;

$$\frac{1}{\pi}\int_a^b g(t)\left\{\frac{1}{t-x}-\frac{\beta}{2}\log|t-x|+\frac{2\pi}{c_0}e^{\beta(t-x)/2}\times\sum_{k=-1}^{2}a_k\left(\frac{\pi}{c}\right)^k S_k\left(-\pi\frac{t+x}{c},0\right)+\frac{\pi}{c}+k_f(x,t)\right\}dt=-p(x)\frac{1+\kappa}{4\mu(x)}. \tag{55}$$

Before closing the formulation, we should note that using the crack displacement itself rather than its derivative such as in Schulze and Erdogan (1998) or following a Fourier Transform-superposition approach such as in Rizk (2003) circumvents this problem about boundary condition (14.a).

4. Numerical solution and stress intensity factors

Singular integral Eq. (55) can be solved by using a series expansion-collocation method. Introducing non-dimensional variables r and s such that $-1\leqslant r,\ s\leqslant 1$, the interval $[a,b]$ can be normalized by defining

$$t=\frac{b-a}{2}r+\frac{b+a}{2},\quad x=\frac{b-a}{2}s+\frac{b+a}{2}, \tag{56}$$

$$g(x(s))=\widehat{G}(s). \tag{57}$$

The unknown function $\widehat{G}(s)$ can be expressed as

$$\widehat{G}(s)=\varphi(s)(1-s)^{\alpha}(1+s)^{\beta}, \tag{58}$$

where $\alpha=\beta=-1/2$ for imbedded cracks and $\alpha=-1/2$, $\beta=0$ for edge cracks ($a=0$). The solution method used by Dag and Erdogan (2002) is adopted in this study. According to this method, the unknown function is expressed in terms of an infinite series of Jacobi polynomials as follows:

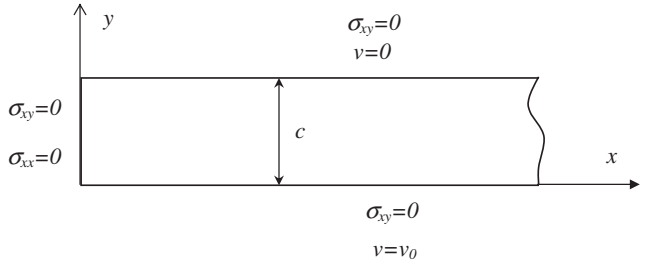

Fig. 2. Semi-infinite FGM strip.

$$\varphi(r)=\sum_{n=0}^{\infty}C_n P_n^{(\alpha,\beta)}(r). \tag{59}$$

The normalized singular integral equation can be regularized by using (57)–(59). Then, truncating the infinite series (59) at a sufficiently large integer N, and using collocation method, an algebraic system of equations can be obtained for the unknown coefficients C_n. For imbedded crack problems, single valuedness condition (48) must also be used. Once C_n are determined, one can express the SIFs for the imbedded crack case as,

$$k_1(a)=\lim_{x\to a-}\sqrt{2(a-x)}\sigma_{yy}(x,0)=\frac{4\mu(-1)}{\kappa+1}\sqrt{\frac{b-a}{2}}\varphi(-1), \tag{60.a}$$

$$k_1(b)=\lim_{x\to b+}\sqrt{2(x-b)}\sigma_{yy}(x,0)=-\frac{4\mu(+1)}{\kappa+1}\sqrt{\frac{b-a}{2}}\varphi(+1), \tag{60.b}$$

and the edge crack case as,

$$k_1(b)=\lim_{x\to b+}\sqrt{2(x-b)}\sigma_{yy}(x,0)=-\frac{4\mu(+1)}{\kappa+1}\sqrt{b}\varphi(+1). \tag{61}$$

5. Finite element implementation

In order to verify the results, some cases are also solved by using FEM. Commercial software ANSYS is used in the calculations. The unit cell shown in Fig. 1 was modeled. Triangular form of PLANE183, 8-noded quadratic elements are used in the mesh, which contains 126455 elements and 255426 nodes. Spatial variations of material properties are implemented through an APDL code (Ansys Parametric Design Language) by assigning the correct values of the material properties at the centroids of each element. To have a perfect match with the analytic solution, loads are applied as crack surface tractions (except constant strain loading), and the other boundary conditions are also implemented similar to the analytic solution. Length of the unit cell is taken as $6\times b$ to simulate the infinite strip boundary condition. Choosing a longer strip would result in very large values of material properties in the model, causing instabilities and inaccurate results. On the other hand, choosing a smaller length results in free surface effects. Thus appropriate length was chosen after some trial and error.

Following Barsoum (1976), special elements are used at the crack tip, which display the correct strain singularity. This is achieved by collapsing the quadrilateral elements into triangular ones by bringing together two corner nodes and then, by shifting the mid-side nodes to the quarter points. Side length of the crack tip elements is taken as $b/1000$ and 12 elements are used around the crack tip. SIFs are computed using Displacement Correlation Technique.

In the transient thermal stress analysis, the same geometry and the mesh are used as in the mechanical analysis. For the stress calculations thickness of the crack free plate is assumed unity and vertical displacements are fixed to zero at the bottom and top edges. Time step is taken as $D/50$. Using larger time steps resulted in non-converging results. T_a is taken as 1.25 and T_0 is taken as 2 units. Reference temperature is also taken as T_0. Two steps are followed for the solution (1) Transient thermal temperatures are calculated as a function of time and written into thermal result file. (2) Element type is switched to structural type and these temperatures are used as loads at the given time.

6. Results and discussion

Results of this study are the SIFs which are calculated for different values of nonhomogeneity parameters, for different crack configurations and for different loadings. Plane strain conditions are considered and $\kappa=2$ (corresponding to Poisson ratio, $\nu=0.25$) is

used in all the calculations. Emphasis is placed on edge cracks since, actually that is the only practical case. Nevertheless, some imbedded crack results under uniform crack surface tractions are also presented for comparison purposes. For imbedded cracks normalized SIFs are given as

$$k^*(a) = \frac{k(a)}{\sigma_0\sqrt{(b-a)/2}}, k^*(b) = \frac{k(b)}{\sigma_0\sqrt{(b-a)/2}}, \tag{62}$$

where σ_0 is the applied uniform crack surface load.

Imbedded crack results are shown graphically in Figs. 3 and 4. In these figures, variation of SIFS with respect to $\ell/(\ell+2c)$ are given where $\ell = b-a$ and $\ell/a = 1.0$. One should note that the curves corresponding to the case of homogeneous material is virtually the same as those given in Nied (1987). The results have also been compared with the corresponding case given in Murakami (1987), in Table 1. A very good agreement is observed. For comparison purposes, FEM results are also obtained for various $b\beta$ values and the agreement between analytic and FEM results are found to be excellent. Thus, FEM results are not shown separately on these figures.

For edge cracks, three distinct loading cases are considered. In the first case, following Dag and Erdogan (2002), crack surface tractions are taken as proportional to powers of x (up to the order three), which can be expressed as follows:

$$p(x) = \sigma_0 \times \left(\frac{x}{b}\right)^k, \quad k = 0,1,2,3. \tag{63}$$

By superposing the SIFs obtained using these crack surface tractions for different powers of x, fairly general loading conditions on the FGM half-plane could be implemented. Normalized SIFs for edge cracks are defined as

$$k^*(b) = \frac{k(b)}{\sigma_0\sqrt{b}}. \tag{64}$$

Comparisons are made with the corresponding case in Murakami (1987) for edge cracks as well, where the results are read from a plot. Note that since the formulation in this article is made for FGM materials, it becomes degenerate for homogeneous ($b\beta = 0$ exactly) materials. So, calculations for homogeneous materials are done by taking $b\beta = -10^{-4}$ or $b\beta = 10^{-4}$ which produce the same results (Table 2). Variation of mode I SIFs with respect to crack spacing for various values of nonhomogeneity parameter are given in Tables 3–6 for power law type of crack surface tractions. For uniform stress loading FEM results are also included in Table 3 (boldface values) where an excellent agreement between analytic and FEM results is observed. In these tables, the last row corresponds to a single crack case, and the values are taken from Dag and Erdogan (2002). The middle column with zero nonhomogeneity parameter corresponds to a homogeneous half space. To facilitate comparison with (Nied, 1987) where the results were presented in graphical form, analytic SIFs under uniform stress loading versus crack spacing for various values of nonhomogeneity parameters is given in Fig. 5. The middle curve in this figure represents homogeneous material. A very good agreement is observed between our results and those given in Nied (1987) for this case as well. This family of curves summarize the general trends very well. For a wide range of crack spacings, ($b/(b+2c) > 0.15$) SIFs increase as $b\beta$ increases from -3 to 3, thus bracketing the SIFs of a homogeneous half plane, for a given crack spacing. For widely spaced cracks, however, smaller $b\beta$ values give larger SIFs. From the results, it can be observed that, *i*) decreasing crack spacing reduces the SIFs significantly for the whole range of $b\beta$ values, and *ii*) for negative $b\beta$ values (reducing stiffness in x direction) , this reduction is still significant at relatively large crack spacings. For example from Table 3, the single crack SIF is reached for $c/b = 4$ when $b\beta$ is equal to 3.0, but for $b\beta = -3.0$, even at $c/b = 10$, the periodic SIFs are still less than half of the single crack SIF.

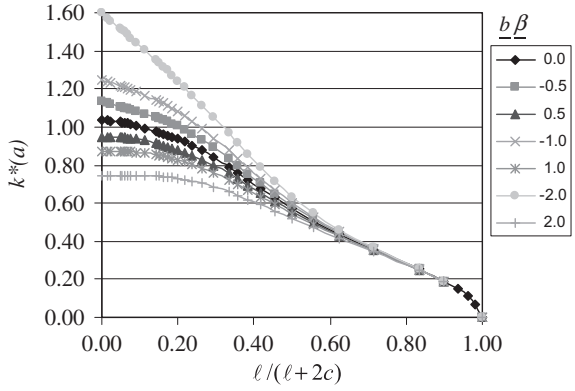

Fig. 3. Stress intensity factors at a for an imbedded crack under uniform loading.

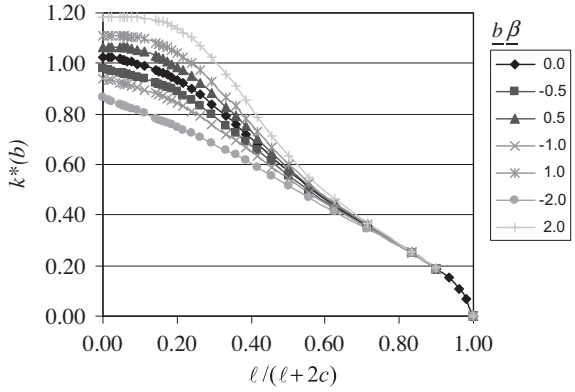

Fig. 4. Stress intensity factors at b for an imbedded crack under uniform loading.

Table 1
Comparison of $k(a)/\sigma_0\sqrt{(b-a)/2}$ for an internal crack with the corresponding case in Murakami (1987).

$(b-a)/(b+a)$	$(b-a)/(4c)$	(Murakami, 1987)	Current study
0.5	0.0	1.0914	1.0913
	0.1	0.9888	0.9888
	0.2	0.8594	0.8594
	0.333	0.7089	0.7087
	0.5	0.5735	0.5729
0.333	0.0	1.0346	1.0345
	0.1	0.9608	0.9609
	0.2	0.8528	0.8528
	0.333	0.7015	0.7012
	0.5	0.5708	0.5702

Table 2
Comparison of $k(b)/\sigma_0\sqrt{b}$ for an edge crack with the corresponding case in Murakami (1987).

$2c/b$	Murakami (1987)	Current study $\beta b = -10^{-4}$	Current study $\beta b = 10^{-4}$
1.03	0.400	0.4042	0.4043
2.00	0.561	0.5581	0.5581
4.00	0.791	0.7934	0.7934
6.00	0.929	0.9288	0.9288
8.00	0.997	0.9996	0.9996

Table 3
Normalized stress intensity factors under uniform crack surface traction σ_0 for an edge crack.

$k(b)/\sigma_0\sqrt{b}$										
c/b	$b\beta$	−3.0	−2.0	−1.0	−0.5	0.0	0.5	1.0	2.0	3.0
0.00		0	0	0	0	0	0	0	0	0
0.10		0.1743	0.1757	0.1772	0.1779	0.1786	0.1794	0.1801	0.1816	0.1831
		0.1739	**0.1753**	**0.1769**	**0.1777**	**0.1785**	**0.1793**	**0.1801**	**0.1817**	**0.1833**
0.30		0.2853	0.2930	0.3009	0.3050	0.3090	0.3132	0.3173	0.3259	0.3349
		0.2849	**0.2927**	**0.3006**	**0.3046**	**0.3087**	**0.3128**	**0.3170**	**0.3256**	**0.3345**
0.50		0.3501	0.3657	0.3817	0.3900	0.3987	0.4078	0.4175	0.4392	0.4643
		0.3499	**0.3655**	**0.3815**	**0.3898**	**0.3985**	**0.4076**	**0.4173**	**0.4390**	**0.4641**
0.70		0.3976	0.4189	0.4418	0.4548	0.4695	0.4862	0.5050	0.5490	0.5997
		0.3974	**0.4187**	**0.4416**	**0.4546**	**0.4693**	**0.4860**	**0.5048**	**0.5487**	**0.5995**
1.00		0.4491	0.4743	0.5077	0.5305	0.5581	0.5900	0.6251	0.6996	0.7720
		0.4486	**0.4739**	**0.5072**	**0.5300**	**0.5575**	**0.5893**	**0.6245**	**0.6989**	**0.7712**
2.00		0.5405	0.5829	0.6739	0.7345	0.7934	0.8425	0.8801	0.9316	0.9662
		0.5408	**0.5834**	**0.6744**	**0.7351**	**0.7940**	**0.8431**	**0.8807**	**0.9323**	**0.9669**
4.00		0.6388	0.7437	0.9250	0.9872	0.9996	0.9889	0.9807	0.9787	0.9880
		0.6385	**0.7434**	**0.9246**	**0.9868**	**0.9992**	**0.9890**	**0.9803**	**0.9782**	**0.9802**
10.0		0.8430	1.1094	1.3123	1.2423	1.0990	1.0213	0.9930	0.9806	0.9884
		0.8355	**1.0998**	**1.2992**	**1.2305**	**1.0892**	**1.0037**	**0.9808**	**0.9799**	**0.9806**
∞ (Dag and Erdogan, 2002)		4.4345	3.1238	1.9843	1.4989	1.1215	1.0225	0.9932	0.9807	0.9884

Table 4
Normalized stress intensity factors under linear crack surface traction $\sigma_0(x/b)$ for an edge crack.

$k(b)/\sigma_0\sqrt{b}$										
c/b	$b\beta$	−3.0	−2.0	−1.0	−0.5	0.0	0.5	1.0	2.0	3.0
0.00		0	0	0	0	0	0	0	0	0
0.10		0.1713	0.1727	0.1741	0.1748	0.1755	0.1762	0.1769	0.1784	0.1798
0.30		0.2706	0.2777	0.2850	0.2888	0.2926	0.2965	0.3005	0.3088	0.3176
0.50		0.3216	0.3349	0.3487	0.3559	0.3633	0.3710	0.3790	0.3961	0.4146
0.70		0.3559	0.3732	0.3910	0.4005	0.4105	0.4213	0.4329	0.4581	0.4849
1.00		0.3916	0.4097	0.4300	0.4422	0.4562	0.4718	0.4884	0.5224	0.5542
2.00		0.4488	0.4663	0.5023	0.5270	0.5515	0.5722	0.5883	0.6103	0.6249
4.00		0.4987	0.5335	0.6019	0.6273	0.6336	0.6304	0.6279	0.6282	0.6328
10.0		0.5840	0.6767	0.7547	0.7291	0.6737	0.6435	0.6328	0.6289	0.6329
∞ (Dag and Erdogan, 2002)		1.9324	1.4495	1.0196	0.8317	0.6829	0.6439	0.6328	0.6289	0.6329

Table 5
Normalized stress intensity factors under parabolic crack surface traction $\sigma_0(x/b)^2$ for an edge crack.

$k(b)/\sigma_0\sqrt{b}$										
c/b	$b\beta$	−3.0	−2.0	−1.0	−0.5	0.0	0.5	1.0	2.0	3.0
0.00		0	0	0	0	0	0	0	0	0
0.10		0.1683	0.1697	0.1710	0.1717	0.1724	0.1731	0.1738	0.1752	0.1767
0.30		0.2574	0.2637	0.2703	0.2736	0.2771	0.2806	0.2841	0.2915	0.2992
0.50		0.2982	0.3091	0.3204	0.3262	0.3322	0.3383	0.3446	0.3578	0.3717
0.70		0.3237	0.3374	0.3511	0.3583	0.3657	0.3736	0.3817	0.3989	0.4166
1.00		0.3496	0.3634	0.3779	0.3862	0.3954	0.4054	0.4159	0.4368	0.4560
2.00		0.3898	0.4005	0.4214	0.4358	0.4503	0.4626	0.4722	0.4853	0.4939
4.00		0.4223	0.4400	0.4781	0.4930	0.4971	0.4957	0.4945	0.4952	0.4982
10.0		0.4724	0.5210	0.5649	0.5512	0.5202	0.5032	0.4973	0.4956	0.4982
∞ (Dag and Erdogan, 2002)		1.2148	0.9525	0.7152	0.6099	0.5255	0.5035	0.4974	0.4956	0.4981

The second loading case is constant strain loading where a uniform strain ε_0 is imposed in y-direction. For this case, the crack surface tractions can be expressed as

$$p(x) = \frac{2\mu(x)\varepsilon_0}{1-\nu}, \tag{65}$$

and the normalized SIFs are given as

$$k^*(b) = k(b)/\left(\frac{2\mu_0\varepsilon_0}{1-\nu}\sqrt{b}\right). \tag{66}$$

Here one should observe that ε_{xx} is non zero for the assumed elasticity solution, and straining in y-direction has been accomplished without putting any constraint on the deformation in x-direction. Results of constant strain loading are given in Table 7. Here again FEM results are shown in bold face letters and a very good agreement with analytic results is obtained, only slightly deteriorating for large c/b and βb values. It is observed that, as the nonhomogeneity parameter increases from −3 to 3, SIFs also increase except for very large crack spacings (or practically single crack case). For

Table 6
Normalized stress intensity factors under cubic crack surface traction $\sigma_0(x/b)^3$ for an edge crack.

$k(b)/\sigma_0\sqrt{b}$									
c/b $b\beta$	−3.0	−2.0	−1.0	−0.5	0.0	0.5	1.0	2.0	3.0
0.00	0	0	0	0	0	0	0	0	0
0.10	0.1654	0.1668	0.1681	0.1688	0.1694	0.1701	0.1708	0.1722	0.1735
0.30	0.2457	0.2514	0.2572	0.2601	0.2632	0.2663	0.2694	0.2759	0.2826
0.50	0.2792	0.2884	0.2977	0.3025	0.3074	0.3124	0.3174	0.3279	0.3387
0.70	0.2991	0.3102	0.3212	0.3268	0.3327	0.3386	0.3448	0.3576	0.3704
1.00	0.3189	0.3299	0.3410	0.3472	0.3539	0.3611	0.3686	0.3833	0.3964
2.00	0.3492	0.3568	0.3711	0.3809	0.3908	0.3992	0.4058	0.4147	0.4206
4.00	0.3727	0.3838	0.4089	0.4189	0.4220	0.4212	0.4206	0.4212	0.4233
10.0	0.4069	0.4374	0.4665	0.4578	0.4374	0.4262	0.4224	0.4214	0.4233
∞ (Dag and Erdogan, 2002)	0.8897	0.7209	0.5663	0.4970	0.4410	0.4264	0.4225	0.4215	0.4233

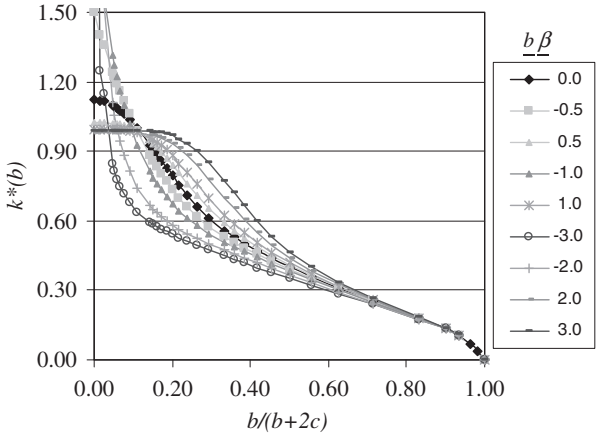

Fig. 5. Stress intensity factors for an edge crack under uniform crack surface traction.

functionally graded half planes with decreasing stiffness in depth direction, there are competing effects of crack spacing and reducing stiffness. When the crack spacing is close, its effect dominate resulting in SIFs lower than that of homogeneous half plane. As the cracks become wide apart, the influence of low stiffness begins to dominate and SIFs for the FGM begin to catch up with those of the homogeneous material. In the limiting case of single crack the SIFs for the FGM become greater than those of the homogeneous material.

The third and final loading case is a cooling thermal shock. For the thermal shock problem, the crack-free half-plane is assumed to be at a uniform temperature T_0, when suddenly, the surface is brought to a lower temperature T_a. For the closed form solution it is assumed that the temperature at infinity is kept at the initial temperature. Dynamic effects are neglected, thus a quasi-static solution is considered. Here, it is assumed that crack opening displacements are small, thus the heat flow in x-direction is not influenced. As such, the problem became a one dimensional, transient conduction problem.

It is assumed that the thermal conductivity is varying along the x-axis as an exponential function,

$$k(x) = k_0 \exp(\delta x), \tag{67}$$

but as a simplifying assumption the thermal diffusivity, $D = k(x)/(c(x)\rho(x))$ is taken as constant. In other words, assuming exponentially varying heat capacity and density,

$$c(x) = c_0 \exp(\eta x), \quad \rho(x) = \rho_0 \exp(\omega x), \tag{68}$$

respectively, the exponents must satisfy the relationship

$$\omega + \eta = \delta, \tag{69}$$

and

$$D = \frac{k_0}{c_0 \rho_0}. \tag{70}$$

Coefficient of thermal expansion for the half plane is also assumed to be an exponential function of x such that,

$$\alpha(x) = \alpha_0 \exp(\xi x). \tag{71}$$

Solution to the conduction problem posed above can be found by using standard Laplace transform techniques. The corresponding thermal stress problem for the crack-free FGM half-plane can also be obtained easily. The resulting temperature distribution and the stress field are given by

$$\frac{\theta(x,t)}{\theta_a} = \exp\left(-\frac{\delta x}{2}\right)\left\{\cosh(2\lambda) - \frac{1}{2}\left[\exp(2\lambda)\mathrm{erf}\left(\frac{u^2+\lambda}{u}\right) + \exp(-2\lambda)\mathrm{erf}\left(\frac{u^2-\lambda}{u}\right)\right]\right\}, \tag{72.a}$$

where,

$$\theta(x,t) = T(x,t) - T_0, \quad \theta_a = T_a - T_0, \quad \lambda = \delta x/4, \quad u = \frac{x}{2\sqrt{Dt}}, \tag{72.b}$$

and the thermal stress is given as

$$\sigma_{yy}(x,t) = -\frac{2(1+\nu)\alpha(x)\mu(x)\theta(x,t)}{1-\nu}. \tag{73}$$

Temperature distribution can also be expressed in terms of non-dimensional variables, which make more physical sense;

$$\delta_b = \delta.b, \quad x_b = x/b, \quad Fo = D.t/b^2 \tag{74}$$

which are the conduction nonhomogeneity, the normalized position, and the Fourier number (non-dimensional time), respectively. To obtain sample results, the cases shown in Table 8 have been investigated. Case 3 is a homogeneous material. Case 1 and Case 2 are hypothetical materials. In case 1, by choosing positive exponents, increasing Young's modulus, conduction coefficient and coefficient of thermal expansion have been assumed. Qualitatively speaking, some ceramic-metal FGMs, (ceramic on the surface, becoming increasingly metal rich in x-direction) might have a property variation like this, since ceramics typically have a much lower coefficient of conduction and a moderately lower coefficient of thermal expansion. (For some ceramic metal systems though, metal might have lower Young's modulus.) Hence case 1 is considered to be a more realistic one. Case 2 is basically intended to demonstrate the trend of SIF while going from positive exponents, through homogeneous material to negative exponents. For the crack problem, opposite of the thermal stress given in (73) is applied as the crack face pressure. For this case, the SIFs are normalized as,

Table 7
Normalized stress intensity factors under constant strain loading for an edge crack.

$k(b)/\left(\frac{2\mu_0\varepsilon_0}{1-\nu}\sqrt{b}\right)$										
c/b	$b\beta$	−3.0	−2.0	−1.0	−0.5	0.0	0.5	1.0	2.0	3.0
0.00		0	0	0	0	0	0	0	0	0
0.10		0.0091	0.0246	0.0663	0.1089	0.1786	0.2931	0.4810	1.2953	3.4879
		0.0091	**0.0246**	**0.0662**	**0.1087**	**0.1785**	**0.2929**	**0.4808**	**1.2955**	**3.4905**
0.30		0.0167	0.0441	0.1168	0.1899	0.3090	0.5028	0.8180	2.1647	5.7279
		0.0167	**0.0441**	**0.1166**	**0.1897**	**0.3087**	**0.5022**	**0.8171**	**2.1624**	**5.7220**
0.50		0.0227	0.0590	0.1533	0.2472	0.3987	0.6429	1.0368	2.6952	7.0000
		0.0227	**0.0590**	**0.1532**	**0.2470**	**0.3985**	**0.6426**	**1.0364**	**2.6939**	**7.0000**
0.70		0.0281	0.0716	0.1832	0.2933	0.4695	0.7515	1.2023	3.0722	7.8323
		0.0281	**0.0716**	**0.1832**	**0.2932**	**0.4693**	**0.7511**	**1.2018**	**3.0709**	**7.8291**
1.00		0.0349	0.0874	0.2208	0.3512	0.5581	0.8850	1.3998	3.4794	8.6160
		0.0349	**0.0874**	**0.2206**	**0.3509**	**0.5575**	**0.8841**	**1.3985**	**3.4760**	**8.6078**
2.00		0.0525	0.1317	0.3322	0.5184	0.7934	1.1957	1.7904	4.0471	9.4006
		0.0525	**0.1318**	**0.3325**	**0.5187**	**0.7940**	**1.1966**	**1.7919**	**4.0535**	**9.4223**
4.00		0.0818	0.2112	0.5067	0.7273	0.9996	1.3760	1.9447	4.1627	9.4884
		0.0818	**0.2111**	**0.5066**	**0.7270**	**0.9992**	**1.3758**	**1.9471**	**4.1817**	**9.5346**
10.0		0.1594	0.4006	0.7765	0.9380	1.0990	1.4158	1.9637	4.1675	9.4898
		0.1569	**0.3967**	**0.7690**	**0.9288**	**1.0920**	**1.4193**	**1.9817**	**4.1904**	**9.6443**
∞		1.6673	1.4582	1.2449	1.1500	1.1215	1.4174	1.9640	4.1685	9.4933

Table 8
Sample data for thermal loading case.

Nonhomogeneity parameter	Case 1	Case 2	Case 3
Elastic, β	0.5	−0.5	0.0
Conduction, δ	1.0	−1.0	0.0
Thermal Expansion , ξ	0.5	−0.5	0.0

$$k^*(b) = k(b)/\left(-\frac{2(1+\nu)\mu_0\alpha_0\theta_a}{1-\nu}\sqrt{b}\right). \tag{75}$$

Variations of thermal SIFs as functions of Fo for various crack spacings (c/b) are given in Table 9. To make sure that the computational procedures and the results for temperature distributions, thermal stresses and SIFs are correct, these are also verified through FEM calculations. Excellent agreements are obtained but comparisons are not shown here because of space limitations except thermal SIFS for $Fo = 1$ and $c/b = 1$ which are given in Table 9 (bold face letters). From this table it can again be observed that a certain steady state value is reached at about $Fo = 4$ for all the cases. It is also observed that, when both the stiffness and the coefficient of thermal expansion are increasing functions of x (i.e. case 1), thermal SIFs are larger. It is also observed that smaller crack spacings for a given crack length gives substantially smaller SIFs.

Because of the constant diffusivity assumption, transient SIFs can not be obtained accurately for a half plane whose diffusivity is variable. Yet, the steady state SIFs are correctly and accurately obtained. As one can observe from (73), steady state value of thermal stress at a given x_0 is also its maximum value for a half plane, since the temperature difference $|\theta(x_0,t)|$ is a monotonically increasing function of t. Then the crack surface tractions also increase steadily until attaining their steady state values. Hence the steady state SIF is also the maximum SIF which is the important quantity regarding fracture. There are elegant analytical solutions which takes variation of diffusivity into account such as those given by (Jin and Feng, 2008) and (Guo and Noda, 2010). In this article, however, the simple solution based on constant diffusivity is preferred because it gives the physically important parameter correctly and yet, it is very easy to implement. Finally, note that as $y \to \infty$, material properties appear to become infinite when the exponents in material property equations are positive. Certainly, this is physically not possible. Here, one should interpret the unbounded semi-infinite plane with an edge crack as a finite width strip where the crack size b is much smaller than the strip width h. The very good agreement between our analytic results (obtained for a semi-infinite plane) and FEM results (which are actually obtained for a finite width layer with a free boundary at the far side) verifies this point.

Table 9
Normalized thermal stress intensity factors for an edge crack.

$k^*(b) = k(b)/\left(-\frac{2(1+\nu)\mu_0\alpha_0\theta_a}{1-\nu}\sqrt{b}\right)$											
Case	c/b	Fo	0.2	0.4	0.6	1.0	1.4	1.8	2.5	3.0	4.0
1	0.20		0.051	0.110	0.145	0.185	0.206	0.219	0.232	0.238	0.245
	1.00		0.187	0.313	0.384	0.460	0.500	0.524	0.549	0.560	0.572
						0.458					
	8.00		0.463	0.645	0.743	0.846	0.900	0.932	0.965	0.979	0.996
2	0.20		0.019	0.041	0.054	0.069	0.077	0.082	0.087	0.089	0.092
	1.00		0.075	0.125	0.153	0.183	0.199	0.209	0.219	0.223	0.228
						0.182					
	8.00		0.393	0.495	0.547	0.602	0.630	0.647	0.664	0.671	0.680
3	0.20		0.032	0.071	0.096	0.125	0.142	0.154	0.168	0.175	0.185
	1.00		0.122	0.208	0.258	0.316	0.350	0.373	0.399	0.413	0.431
						0.315					
	8.00		0.418	0.561	0.640	0.729	0.780	0.814	0.853	0.873	0.901

7. Conclusion

In this paper, a plane elasticity problem, namely, periodic cracking of an FGM half plane under various loading conditions has been considered. Problem is formulated by using Fourier integrals, Fourier series and the derivative of the crack face displacement as an auxiliary unknown. The issues that may arise from the implementation of zero displacement boundary condition along the crack axis (outside the crack) in this type of formulations is pointed out. The problem has been reduced to a singular integral equation with Cauchy type singularity and the SIFs are calculated. These results are also verified through FEM calculations. It is found that

- decreasing crack spacing decreases SIFs significantly for all loading types as pointed out in earlier studies such as Nied (1987), Schulze and Erdogan (1998).

In the first group of results, SIFs for uniform, linear, parabolic and cubic crack surface tractions are presented. Although by themselves SIFs for these cases are not physically meaningful, SIFS for fairly general loading conditions such as uniform stress loading at infinity or thermal SIFS for different types of thermal loadings can be obtained by appropriately superposing these results.

Physically more meaningful results are for the constant strain loading which to some extent represent the fixed grip loading of an FGM strip containing an edge crack where the crack size b is much smaller than the strip width h . The forthcoming conclusions pertain to constant strain loading case. It is found that

- reduction in SIFs at small crack spacings is more significant for functionally graded half planes with increasing stiffness in the depth direction,
- for stiffening half planes, SIFs are higher than those of a homogeneous half plane and higher the stiffening rate, the greater the SIF,
- for softening half planes, SIFs are lower than those of a homogenous half plane except for very large crack spacings (practically the single crack case).

Finally, thermal shock problem under the assumption of constant thermal diffusivity has been considered. It is observed that, for a stiffening half plane with increasing coefficient of thermal expansion, transient thermal SIFs are greater than those of a homogeneous half plane, and for a softening half plane with decreasing coefficient of thermal expansion, transient thermal SIFs are lower than those of a homogeneous half plane.

References

Afsar, A.M., Sekine, H., 2000. Crack spacing effect on the brittle fracture characteristics of semi-infinite functionally graded materials with periodic edge cracks. Int. J. Fract. 102, L61–L66.

Bao, G., Wang, L., 1995. Multiple cracking in functionally graded ceramic/metal coatings. Int. J. Solids Struct. 32, 2853–2871.

Barsoum, R.S., 1976. On the use of isoparametric finite elements in linear fracture mechanics. Int. J. Numer. Methods Eng. 10, 25–37.

Benthem, J.P., Koiter, W.T., 1973. Asymptotic approximations to crack problems. In: Sih, G.C. (Ed.), Mechanics of Fracture, Methods of Analysis and Solutions of Crack Problems, vol. 1. Noordhoof International Publishing, Leyden, The Netherlands, pp. 131–178.

Bowie, O.L., 1973. Solutions of plane crack problems by mapping technique. In: Sih, G.C. (Ed.), Mechanics of Fracture, Methods of Analysis and Solutions of Crack Problems, vol. 1. Noordhoof International Publishing, Leyden, The Netherlands, pp. 1–55.

Chen, J., 2006. Anti-plane problem of periodic cracks in a functionally graded coating-substrate structure. Arch. Appl. Mech. 75, 138–152.

Choi, H.J., 1997. A periodic array of cracks in a functionally graded nonhomogeneous medium loaded under in-plane normal and shear. Int. J. Fract. 88, 107–128.

Dag, S. 1997. Crack Problems in a Functionally Graded Layer under Thermal Stresses. MS Thesis, Middle East Technical University, Ankara, Turkey

Dag, S., Erdogan, F., 2002. A surface crack in a graded medium under general loading conditions. ASME J. Appl. Mech. 69, 580–588.

Dag, S., Yildirim, B., Erdogan, F., 2008. Three dimensional analysis of periodic cracking in fgm coatings under thermal stresses. AIP Conf. Proc. Multiscale and Functionally Graded Materials 2006 973, 676–681.

Ding, S.H., Li, X., 2008. Anti-plane problem of periodic interface cracks in a functionally graded coating-substrate structure. Int. J. Fract. 153, 53–62.

Erdogan, F., 1995. Fracture mechanics of functionally graded materials. Compos. Eng. 5, 753–770.

Erdogan, F., Ozturk, M., 1995. Periodic cracking of functionally graded coatings. Int. J. Eng. Sci. 33, 2179–2195.

Feng, Y.Z., Jin, Z.H., 2009. Thermal fracture of functionally graded plate with parallel surface cracks. Acta Mech. Solida Sinica 22, 453–464.

Guo, L.C., Noda, N., 2010. An analytical method for thermal stresses of a functionally graded material cylindrical shell under a thermal shock. Acta Mech. 214, 71–78.

Han, J.C., Wang, B.L., 2006. Thermal shock resistance enhancement of functionally graded materials by multiple cracking. Acta Mater. 54, 963–973.

Isida, M., 1979. Tension of a half plane containing array cracks, branched cracks and cracks emanating from sharp Notches. Trans. Japan Soc. Mech. Eng. 45 (392), 306–317.

Jin, Z.H., Feng, Y.Z., 2008a. Effects of multiple cracking on the residual strength behavior of thermally shocked functionally graded ceramics. Int. J. Solids Struct. 45, 5973–5986.

Jin, Z.H., Feng, Y.Z., 2008b. Thermal fracture resistance of a functionally graded coating with periodic edge cracks. Surf. Coat. Technol. 202, 4189–4197.

Jin, Z.H., Feng, Y.Z., 2009. An array of parallel edge cracks with alternating lengths in a strip subjected to a thermal shock. J. Therm. Stress. 32, 431–447.

Kadioglu, S., Dag, S., Yahsi, O.S., 1998. Crack problem for a functionally graded layer on an elastic foundation. Int. J. Fract. 94, 63–77.

Murakami, Y., 1987. Stress Intensity Factors Handbook. Pergamon Press, Oxford, New York Tokyo.

Nemat-Nasser, S., Keer, L.M., Parihar, K.S., 1978. Unstable growth of thermally induced interacting cracks in brittle solids. Int. J. Solids Struct. 14, 409–430.

Nied, H.F., 1987. Periodic array of cracks in a half-plane subjected to arbitrary loading. ASME J. Appl. Mech. 45, 642–648.

Nisitani, H., Suematu, M., Saito, K., 1973. Tension of a semi-infinite plate with a row of elliptical holes (including cracks) or an infinite plate with two rows of elliptical holes, Trans. Japan. Soc. Mech. Eng. 39 (324), 2323–2330.

Rizk, A.A., 2003. Transient stress intensity factors for periodic array of cracks in a half-plane due to convective cooling. J. Therm. Stress. 26, 443–456.

Rizk, A.A., 2005. Convective thermal shock of an infinite plate with periodic edge cracks. J. Therm. Stress. 28, 103–119.

Rizk, A.A., 2006. An elastic strip with periodic surface cracks under thermal shock. Int. J. Eng. Sci. 44, 807–818.

Schulze, G.W., Erdogan, F., 1998. Periodic cracking of elastic coatings. Int. J. Solids Struct. 35, 3615–3634.

Ueda, S., 2002. Transient thermal singular stresses of multiple cracking in a w-cu functionally graded divertor plate. J. Therm. Stress. 25, 83–95.

Wang, B.L., Mai, Y.W., 2005. A periodic array of cracks in a functional graded materials subjected to thermo-mechanical loading. Int. J. Eng. Sci. 43, 432–446.

Wang, B.L., Mai, Y.W., 2006a. Periodic antiplane cracks in graded coatings under static or transient loading. ASME J. Appl. Mech. 73, 134–142.

Wang, B.L., Mai, Y.W., 2006b. A periodic array of cracks in functionally graded materials subjected to transient loading. Int. J. Eng. Sci. 44, 351–364.

Wang, B.L., Mai, Y.W., 2007. On thermal shock behavior of functionally graded materials. J. Therm. Stress. 30, 523–558.